

## **TECHNICAL REPORT: CVEL-14-066**

### **Modeling the Loading Impedance on Differential-Mode Signals Due to Radiated Emissions**

Li Niu<sup>1</sup>, Todd Hubing<sup>1</sup> and Takehiro Takahashi<sup>2</sup>

<sup>1</sup>Clemson University, SC, USA

<sup>2</sup>Takushoku University, Japan

March 1, 2015

---

---

## Table of Contents

Abstract.....	3
1. Introduction.....	3
2. Imbalance Difference Theory .....	4
2.1 Imbalance Factor .....	4
2.2 Conversion Impedance.....	6
3. Experimental Validation.....	7
3.1 Example Structure and Measurement Setup .....	7
3.2 Calculation Procedure .....	9
3.3 Comparison between Calculation Results and Measurement Results .....	11
4. Conclusion .....	14
References.....	14



---

## Abstract

Imbalance difference theory describes the conversion mechanism between differential-mode signals and antenna-mode signals on transmission lines. For unintended radiated emission problems, it provides an easy and yet powerful technique to calculate the antenna-mode current that is converted from differential-mode signals. In this paper, we introduce conversion impedance to the existing imbalance difference theory model to account for the loading effect on the differential-mode circuit, so that when the coupling between differential mode and antenna mode are strong, the imbalance difference theory can more accurately estimate the AM current.

## 1. Introduction

Unintended radiated emission is a challenging problem for high speed electronic devices; it has been known for a long time that it is caused by the unintended antenna mode (AM) currents on the cables or other electrically large metal parts. The AM were frequently referred to in the literatures as common mode (CM). We, however, distinguish them in the way that the CM exhibits TEM propagation while the AM does not and it radiates energy away from the structure.

The intended signals on transmission lines are usually differential mode (DM), the fundamental mechanisms by which differential-mode signals are converted to antenna-mode currents on cables attached to printed circuit boards were first studied in [1]–[3], where these mechanisms were described by current-driven models and voltage-driven models. A more precise and easy-to-apply method called Imbalance Difference Theory (IDT) was introduced later in [4]. IDT pointed out that the unintended antenna-mode current was generated due to a change in the electrical balance of the transmission lines carrying the differential signal currents. The exact antenna-mode current can be accurately calculated based on the transmission line geometries and the strength of the differential-mode signal at the interface.

---

The IDT has been successfully applied to a number of radiated emission problems since its introduction [5]–[17]. However it wasn't rigorously derived until a recently published paper by the author [21], where we demonstrated that if the imbalance factor is defined as the actual current division factor, IDT is strictly correct for radiated emission calculation. We also shown in that paper the conventional method of calculating imbalance factor by analyzing the cross sections of the transmission lines [4] [8] was a very close approximation to the actual current division factor.

For radiated emission problems, the DM and AM signals are usually weakly coupled: only a small portion of the DM energy is converted to AM energy, and the energy converted back to DM is even smaller and can be neglected. For the strong coupling case however, ignoring the energy converted back to DM can affect the accuracy of the calculation. In another recently published paper [22], the IDT was applied to a multi-conductor transmission line structure, where the CM signals exhibit TEM propagation and the DM and CM signals are strongly coupled. We introduced the concept of conversion impedance to the IDT model to account for the loading effect to the original DM circuit due to DM-CM conversion.

In this paper we first explore the conversion impedance of IDT model for radiation emission applications. Then we provide an example calculation to show that when the coupling between DM and AM is strong, i.e. when the structure hit resonant frequency, the conversion impedance has big impact over the accuracy of IDT model.

## **2. Imbalance Difference Theory**

### **2.1 Imbalance Factor**

Consider a two-conductor transmission line with a cross-section that suddenly changes as shown in Fig. 1. At the interface where the cross-section changes, the voltage between the two conductors is  $V_{DM}$ . As described in [21], the change in the electrical balance of the conductors results in an antenna-mode

voltage that drives the conductors on one side of the interface relative to the conductors on the other side of the interface as indicated in Fig. 2. The amplitude of the driving voltage is given by,

$$V_{AM} = \Delta h \cdot (V_{DM}). \quad (1)$$

where  $\Delta h$  is the change in the imbalance factor occurring at the interface and  $V_{DM}$  is the differential-mode voltage at the interface. The imbalance factor of each section of the transmission lines is defined as the ratio of the AM currents on each conductor in Fig. 2.

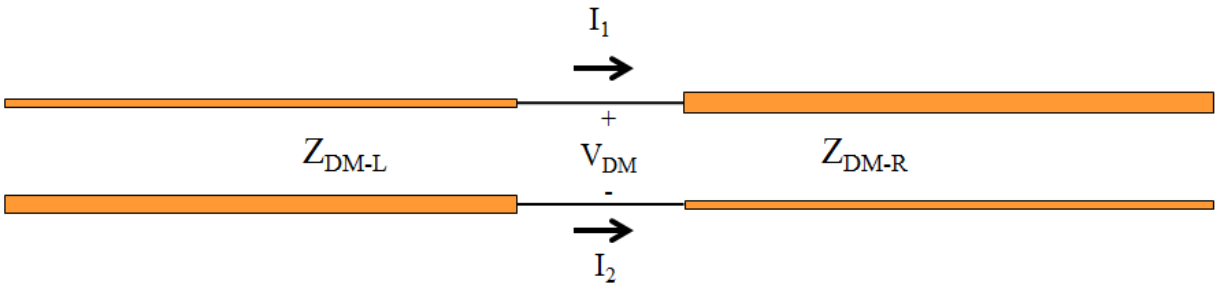


Fig. 1. Two-conductor transmission lines with changed cross-section.

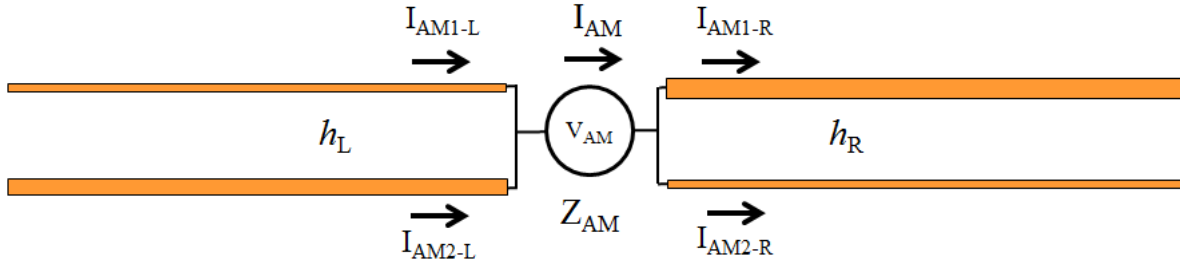


Fig. 2. Antenna mode of TLs with divided AM current.

The imbalance factor for left and right section of the TL,  $h_L$  and  $h_R$  are:

$$h_L = I_{AM1-L} / (I_{AM1-L} + I_{AM2-L}). \quad (2)$$

$$h_R = I_{AM1-R} / (I_{AM1-R} + I_{AM2-R}). \quad (3)$$

The  $I_{AM-1L}$ ,  $I_{AM-2L}$ ,  $I_{AM-1R}$ , and  $I_{AM-2R}$  denote the AM current on each conductor of the TLs in Fig. 2.

For realistic radiated emission applications, the current division factor or imbalance factor is hard to obtain precisely, but [21] demonstrated that expressing  $h$  as a ratio of the per-unit-length inductances or capacitances is a very good approximation. The equations are:

$$h = \frac{C_{11}}{C_{11} + C_{22}}. \quad (4)$$

$$h = \frac{L_{22} - L_{12}}{L_{11} + L_{22} - 2L_{12}}. \quad (5)$$

Detailed definitions of  $C_{11}$ ,  $C_{22}$ ,  $L_{11}$ ,  $L_{22}$  and  $L_{12}$  can be found in [8].

## 2.2 Conversion Impedance

The imbalance difference theory describes a method to calculate the conversion between DM and CM/AM signals [4] [8]. It points out that the conversion from one mode to the other is due to the change of electrical balance along the transmission lines and the strength of the conversion is proportional to the change of the imbalance factor.

Based on IDT, for the circuit in Fig. 1, the generated AM current will be equal to that in Fig. 2 when the AM voltage source is:

$$V_{AM} = V_{DM} \cdot (h_R - h_L). \quad (6)$$

If we denote the input impedance of the antenna that the AM voltage source sees in Fig. 2 as  $Z_{AM}$ , then the AM current is:

$$I_{AM} = V_{AM} / Z_{AM} = V_{DM} \cdot (h_R - h_L) / Z_{AM}. \quad (7)$$

According to the IDT, at the interface where imbalance factor changes, there will also be conversion from AM current to DM current as:

$$\Delta I_{DM} = -I_{AM} \cdot (h_R - h_L) = -V_{DM} \cdot (h_R - h_L)^2 / Z_{AM}. \quad (8)$$

The extra DM current,  $\Delta I_{DM}$ , virtually flows from one conductor to the other at the interface, as shown in Fig. 3. Its effect over the DM circuit can be represented by an impedance, which we call conversion impedance,  $Z_{DA}$ , as shown in Fig. 4.

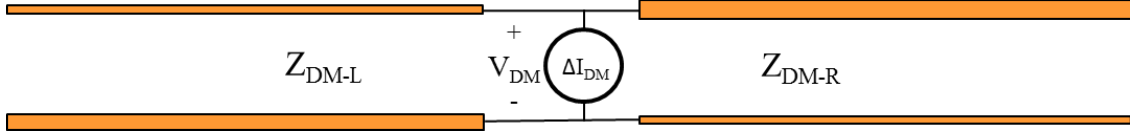


Fig. 3. DM circuit with the extra virtual DM current.

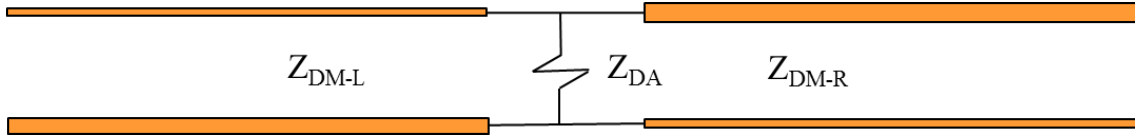


Fig. 4. DM circuit with the conversion impedance.

The expression for the conversion impedance is:

$$Z_{DA} = \frac{V_{DM}}{|\Delta I_{DM}|} = \frac{Z_{AM}}{(h_R - h_L)^2}. \quad (9)$$

### 3. Experimental Validation

#### 3.1 Example Structure and Measurement Setup

As shown in Fig. 5, we connected a twisted wire pair (TWP) to a coaxial cable and kept the structure standing vertically on a metal ground plane. The structure was fed by a DM voltage through underground coaxial cable. The change of electrical balance at the interface between the coaxial cable and the TWP produces AM current. The AM current was measured at the bottom of the antenna close to the ground surface. The feeding DM voltage was measured by an oscilloscope through a T-connector.

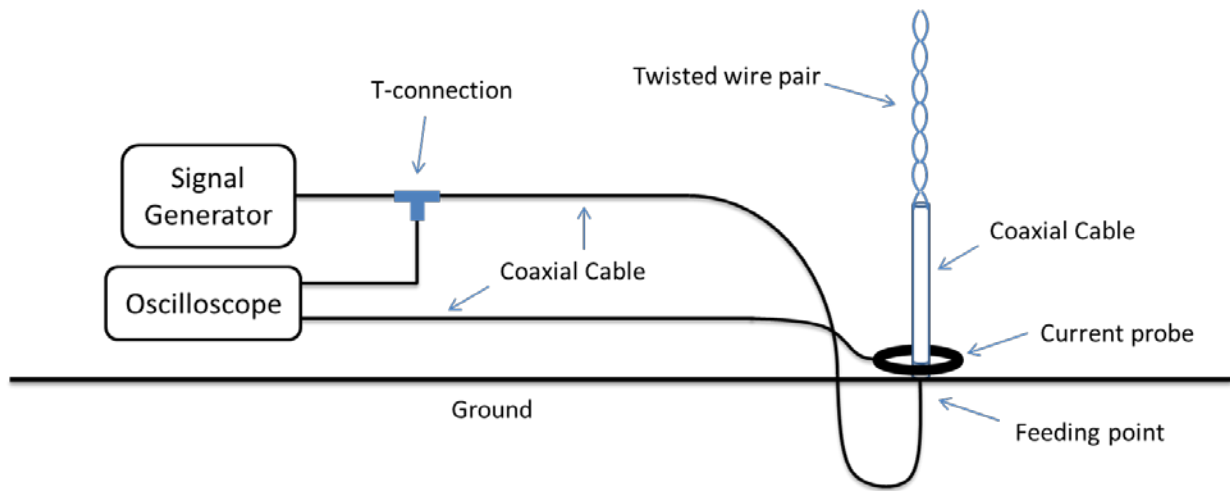


Fig. 5. Validation structure and measurement set up.

Fig. 6 is a photo of the test setup. The tested TWP and coaxial cable were placed in a semi-anechoic chamber and the coaxial cables used for feeding and measurement were placed close to the ground plane so that they had very little effect on the antenna. Measurement set-up parameters are listed in Table. 1.



Fig. 6. Validation structure and measurement set up.



Table. 1. Parameters of measurement setup.

TWP wire	AWG 18 (conductor diameter: 1mm, insulator thickness 0.75mm)
Coaxial cable	RG-58AU
Standing coaxial cable length	0.5 meter
TWP length	0.5 meter
Length of coaxial cable from the feeding point to the T-connection	1.41 meter
Signal generator	BK precision 4087
Oscilloscope	Tektronix MSO 4104
Current probe	Fisher F-33-1
Measured wave velocity of propagation in the TWP	$2.0 \cdot 10^8 \text{ m/s}$
TWP termination	Open circuit

### 3.2 Calculation Procedure

The structure in Fig. 5 can be modeled as the circuit shown in Fig. 7. The goal of the first part of the calculation is to determine the DM voltage at the interface where the TWP and coaxial cable connect so that we can apply IDT to calculate the equivalent AM voltage source that drives the TWP-coaxial-cable antenna.



Fig. 7. Equivalent circuit for measurement set up.

The characteristic impedance of the twisted wire pair,  $Z_{DM-TWP}$  can be calculated by:

$$Z_{DM-TWP} = \frac{120}{\sqrt{\epsilon_r}} \cdot \ln\left(\frac{2 \cdot s}{d}\right). \quad (10)$$

where  $\epsilon_r$  is the relative permittivity of the insulation material;  $s$  is the distance between the centers of two wires,  $d$  is the diameter of the conductor in the wires.

$Z_{DM-Coax}$ ,  $Z_{OSC}$ , and  $Z_{SG}$  are the characteristic impedance of the coaxial cable, the input impedance of the oscilloscope and the output impedance of the signal generator, respectively. They are all  $50\text{ohms}$ . The twisted wire pair is a typical balanced transmission line and the imbalance factor,  $h_{TWP}$ , is 0.5. The coaxial cable is a typical perfectly unbalanced transmission line and the imbalance factor,  $h_{Coax}$ , is 1.

The change of imbalance factor at the interface where TWP connects to the coaxial cable is,

$$\Delta h = h_{Coax} - h_{TWP} = 0.5 . \quad (11)$$

The  $Z_{DA}$  in Fig. 7 is the DM-to-AM conversion impedance. It can be calculated using (9). The input impedance of the antenna was calculated using the antenna modeling software, 4NEC2 [18], where solid wires were used to represent the TWP and the coaxial cable. The equivalent radius used for the coaxial cable was the same as the cable-shield's radius; the one used for the TWP was calculated as [19]:

$$R_{TWP} = \sqrt{s \cdot d / 2} . \quad (12)$$

The input impedance looking into the TWP from the interface is,

$$Z_{in-TWP} = Z_{DM-TWP} \cdot \frac{1}{j \cdot \tan(\beta_{TWP} \cdot l_{TWP})} , \quad (13)$$

where  $l_{TWP}$  is the length of the TWP and  $\beta_{TWP}$  is the phase constant of the TWP.

The load impedance that the coaxial cable sees at the interface is,

$$Z_{L-mid} = Z_{DA} \parallel Z_{in-TWP} . \quad (14)$$

The input impedance looking into the coaxial cable is,

$$Z_{in-Coax} = Z_{DM-Coax} \cdot \frac{Z_{L-mid} + j \cdot Z_{DM-Coax} \cdot \tan(\beta_{Coax} \cdot l_{Coax})}{Z_{DM-Coax} + j \cdot Z_{L-mid} \cdot \tan(\beta_{Coax} \cdot l_{Coax})} . \quad (15)$$

where  $\beta_{coax}$  is the phase constant of the coaxial cable and the  $l_{Coax}$  is the length of the coaxial cable from the interface where it connects to the TWP to the T-connection.

The DM voltage at the T-connection that feeds the coaxial cable can be calculated as,

$$V_{coax-feed} = V_{SG} \cdot \frac{Z_{in-Coax} \parallel Z_{OSC}}{Z_{in-Coax} \parallel Z_{OSC} + Z_{SG}} . \quad (16)$$

The reflection coefficient at the interface where coaxial cable connects to TWP is,

$$\Gamma_{mid} = \frac{Z_{L-mid} - Z_{DM-Coax}}{Z_{L-mid} + Z_{DM-Coax}} . \quad (17)$$

So the positive propagation voltage at the interface is,

$$V_{mid}^+ = \frac{V_{coax-feed}}{e^{j \cdot \beta_{coax} \cdot l_{coax}} + \Gamma \cdot e^{-j \cdot \beta_{coax} \cdot l_{coax}}} . \quad (18)$$

and the DM voltage at the interface is,

$$V_{DM} = V_{mid}^+ + V_{mid}^+ \cdot \Gamma . \quad (19)$$

Applying IDT yields the equivalent AM voltage source that drives the antenna:

$$V_{AM} = V_{DM} \cdot \Delta h . \quad (19)$$

With the equivalent AM voltage source, we build the structure similar as that in 4nec2 in a MOM simulation software, FEKO [20], to calculate the AM current at the bottom of the antenna.

### 3.3 Comparison between Calculation Results and Measurement Results

We calculated the DM voltage that feeds the coaxial cable at the T-connection in Fig. 5 and the AM current at the bottom of the antenna. The IDT was applied both with and without conversion

impedance  $Z_{DA}$ . The comparisons of the calculated results and the measurement results are shown in Fig. 8 and Fig. 9.

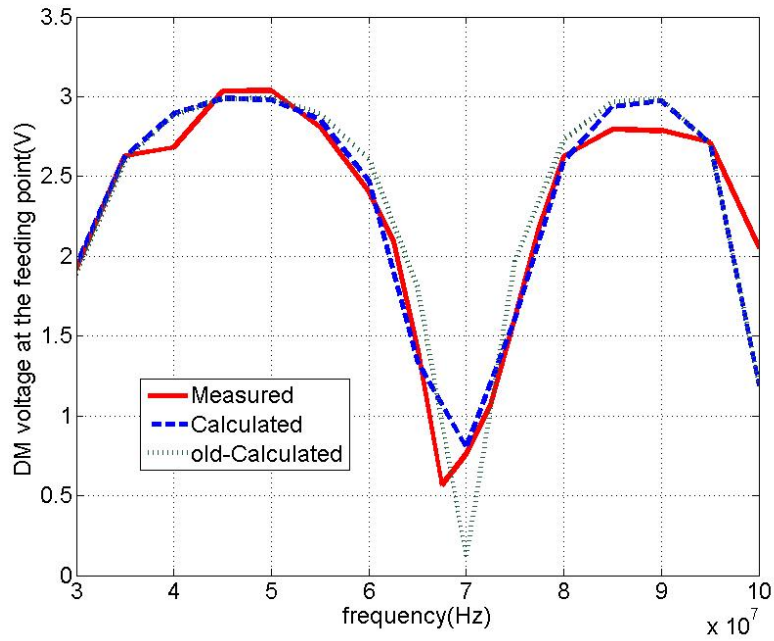


Fig. 8. Comparison of DM voltage at the T-connection.

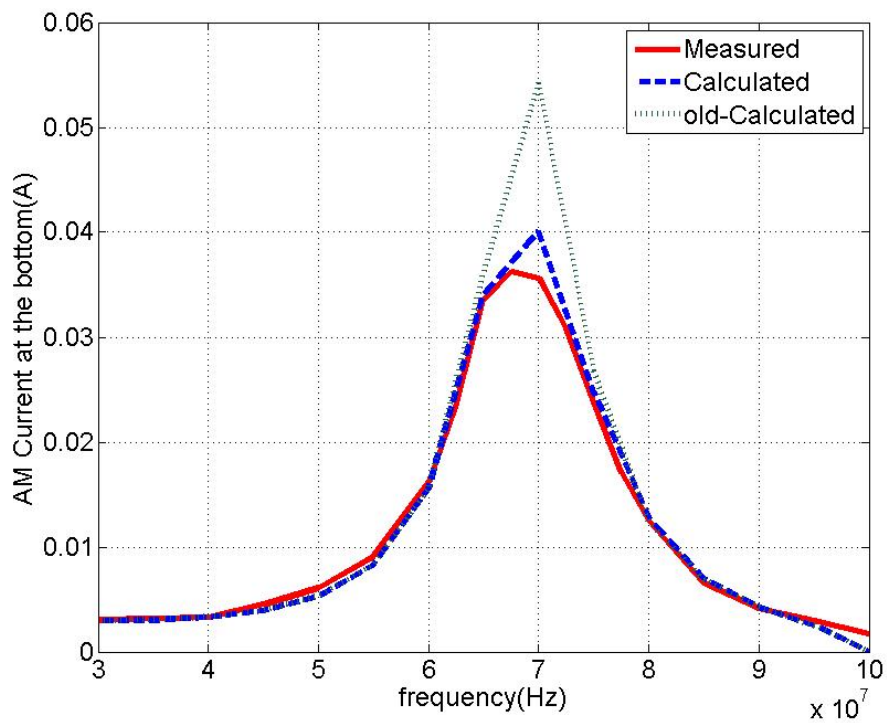


Fig. 9. Comparison of AM current at the bottom of the antenna.

---

We can see from Fig. 8 and Fig. 9 that the calculated results with conversion impedance, labelled as “Calculated” in the plots, are very close to the measurement result over the frequency from 30MHz to 100MHz. The results without conversion impedance, noted as “old-Calculated” in both plots, are very close to that with conversion impedance over most of the frequency range except at resonant frequency, around 70MHz, where the old model over-estimated the AM current.

Here is the explanation: According to (9), the conversion impedance is proportional to the input impedance of the antenna,  $Z_{AM}$ , in our case, it is 4 times of  $Z_{AM}$ . At non-resonant frequencies,  $Z_{AM}$  is about couple hundreds ohms, which can be seen on an input-impedance-over-frequency plot on Fig. 10, so the  $Z_{DA}$  is much bigger than the DM impedances. At resonant frequency, however, the input impedance is about 70 ohms and the  $Z_{DA}$  is less than 300 ohms, which is comparable to the DM impedances, as a result neglecting  $Z_{DA}$  causes less accurate calculation results.

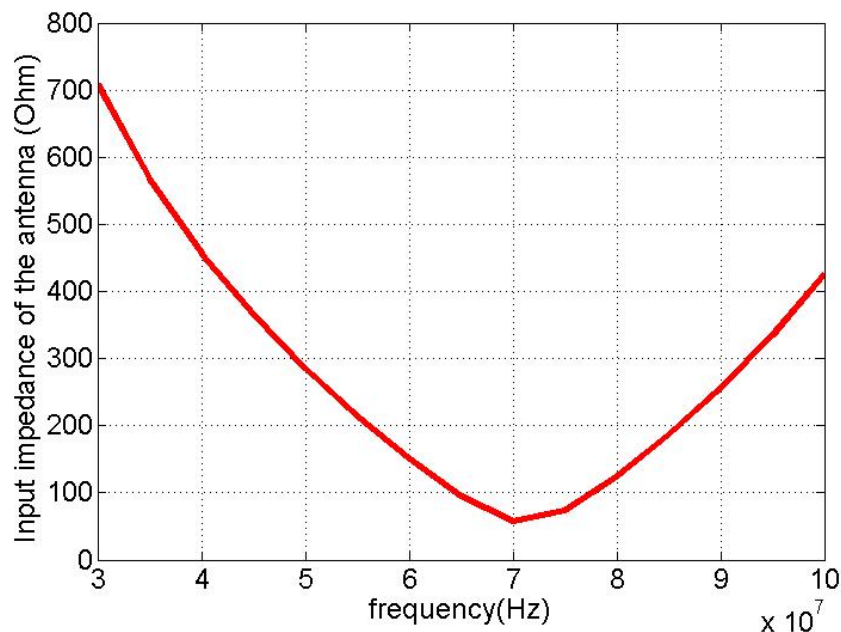


Fig. 10. Input impedance of the antenna seen by the AM voltage source.

---

## 4. Conclusion

In this paper we introduce the conversion impedance to the imbalance difference theory for modelling radiated emissions. For most practical radiating structures, at non-resonant frequencies, the conversion impedance is much larger than the DM impedances in the circuit and it has little impact over the accuracy of IDT models. However, we demonstrate with an example structure that the conversion impedance can have big influence over the accuracy of the IDT model if the radiating structure hits resonant frequency and the conversion impedance becomes comparable to the DM impedances.

## References

- [1] J. L. Drewniak, T. H. Hubing, and T. P. Van Doren, "Investigation of fundamental mechanisms of common-mode radiation from printed circuit boards with attached cables," in *Proceedings of IEEE Symposium on Electromagnetic Compatibility*, 1994, pp. 110–115.
- [2] J. L. Drewniak, T. P. Van Doren, T. H. Hubing, and J. Shaw, "Diagnosing and modeling common-mode radiation from printed circuit boards with attached cables," in *Proceedings of International Symposium on Electromagnetic Compatibility*, 1995, vol. 1, pp. 465–470.
- [3] D. M. Hockanson, J. L. Drewniak, T. H. Hubing, T. P. Van Doren, and M. J. Wilhelm, "Investigation of fundamental EMI source mechanisms driving common-mode radiation from printed circuit boards with attached cables," *IEEE Trans. Electromagn. Compat.*, vol. 38, no. 4, pp. 557–566, 1996.
- [4] T. Watanabe, O. Wada, T. Miyashita, and R. Koga, "Common-Mode-Current Generation Caused by Difference of Unbalance of Transmission Lines on a Printed Circuit Board with Narrow Ground Pattern," *IEICE Trans. Commun.*, vol. E83-B, no. 3, pp. 593–599, Mar. 2000.
- [5] T. Watanabe, O. Wada, Y. Toyota, and R. Koga, "Estimation of common-mode EMI caused by a signal line in the vicinity of ground edge on a PCB," in *IEEE International Symposium on Electromagnetic Compatibility*, 2002, vol. 1, pp. 113–118.
- [6] T. Watanabe, M. Kishimoto, S. Matsunaga, T. Tanimoto, R. Koga, O. Wada, and A. Namba, "Equivalence of two calculation methods for common-mode excitation on a printed circuit board with narrow ground plane," in *2003 IEEE Symposium on Electromagnetic Compatibility. Symposium Record (Cat. No.03CH37446)*, 2003, vol. 1, pp. 22–27.
- [7] O. Wada, "Modeling and simulation of unintended electromagnetic emission from digital circuits," *Electron. Commun. Japan (Part I Commun.)*, vol. 87, no. 8, pp. 38–46, Aug. 2004.
- [8] T. Watanabe, H. Fujihara, O. Wada, R. Koga, and Y. Kami, "A Prediction Method of Common-Mode Excitation on a Printed Circuit Board Having a Signal Trace near the Ground Edge," *IEICE Trans. Commun.*, vol. E87-B, no. 8, pp. 2327–2334, Aug. 2004.
- [9] Y. Toyota, A. Sadatoshi, T. Watanabe, K. Iokibe, R. Koga, and O. Wada, "Prediction of electromagnetic emissions from PCBs with interconnections through common-mode antenna

- 
- model,” in *2007 18th International Zurich Symposium on Electromagnetic Compatibility*, 2007, pp. 107–110.
- [10] Y. Toyota, T. Matsushima, K. Iokibe, R. Koga, and T. Watanabe, “Experimental validation of imbalance difference model to estimate common-mode excitation in PCBs,” in *2008 IEEE International Symposium on Electromagnetic Compatibility*, 2008, pp. 1–6.
- [11] T. Matsushima, T. Watanabe, Y. Toyota, R. Koga, and O. Wada, “Increase of Common-Mode Radiation due to Guard Trace Voltage and Determination of Effective Via-Location,” *IEICE Trans. Commun.*, vol. E92-B, no. 6, pp. 1929–1936, Jun. 2009.
- [12] T. Matsushima, T. Watanabe, Y. Toyota, R. Koga, and O. Wada, “Evaluation of EMI Reduction Effect of Guard Traces Based on Imbalance Difference Model,” *IEICE Trans. Commun.*, vol. E92-B, no. 6, pp. 2193–2200, Jun. 2009.
- [13] C. Su and T. H. Hubing, “Imbalance Difference Model for Common-Mode Radiation From Printed Circuit Boards,” *IEEE Trans. Electromagn. Compat.*, vol. 53, no. 1, pp. 150–156, Feb. 2011.
- [14] H. Kwak and T. H. Hubing, “Investigation of the imbalance difference model and its application to various circuit board and cable geometries,” in *2012 IEEE International Symposium on Electromagnetic Compatibility*, 2012, pp. 273–278.
- [15] T. Matsushima, O. Wada, T. Watanabe, Y. Toyota, and L. R. Koga, “Verification of common-mode-current prediction method based on imbalance difference model for single-channel differential signaling system,” in *2012 Asia-Pacific Symposium on Electromagnetic Compatibility*, 2012, vol. 2, pp. 409–412.
- [16] A. Sugiura and Y. Kami, “Generation and Propagation of Common-Mode Currents in a Balanced Two-Conductor Line,” *IEEE Trans. Electromagn. Compat.*, vol. 54, no. 2, pp. 466–473, Apr. 2012.
- [17] H. Al-Rubaye, K. Pararajasingam, and M. Kane, “Estimating radiated emissions from microstrip transmission lines based on the imbalance model,” in *2012 IEEE Electrical Design of Advanced Packaging and Systems Symposium (EDAPS)*, 2012, pp. 93–96.
- [18] “4nec2.” [Online]. Available: <http://www.qsl.net/4nec2/>.
- [19] C. A. Balanis, “Antenna Theory, Analysis and Design,” 2nd Edition, John Wiley & Sons, Inc. 1997, p. 456.
- [20] *FEKO User’s Manual*, Suite 6.2. 2013.
- [21] L. Niu and T. Hubing, “Rigorous Derivation of Imbalance Difference Theory for Modeling Radiated Emission Problems,” CVEL-14-056, Dec. 20, 2014.
- [22] L. Niu and T. Hubing, “Modeling the Conversion between Differential Mode and Common Mode Propagation in Transmission Lines,” CVEL-14-055, Mar. 1, 2015.